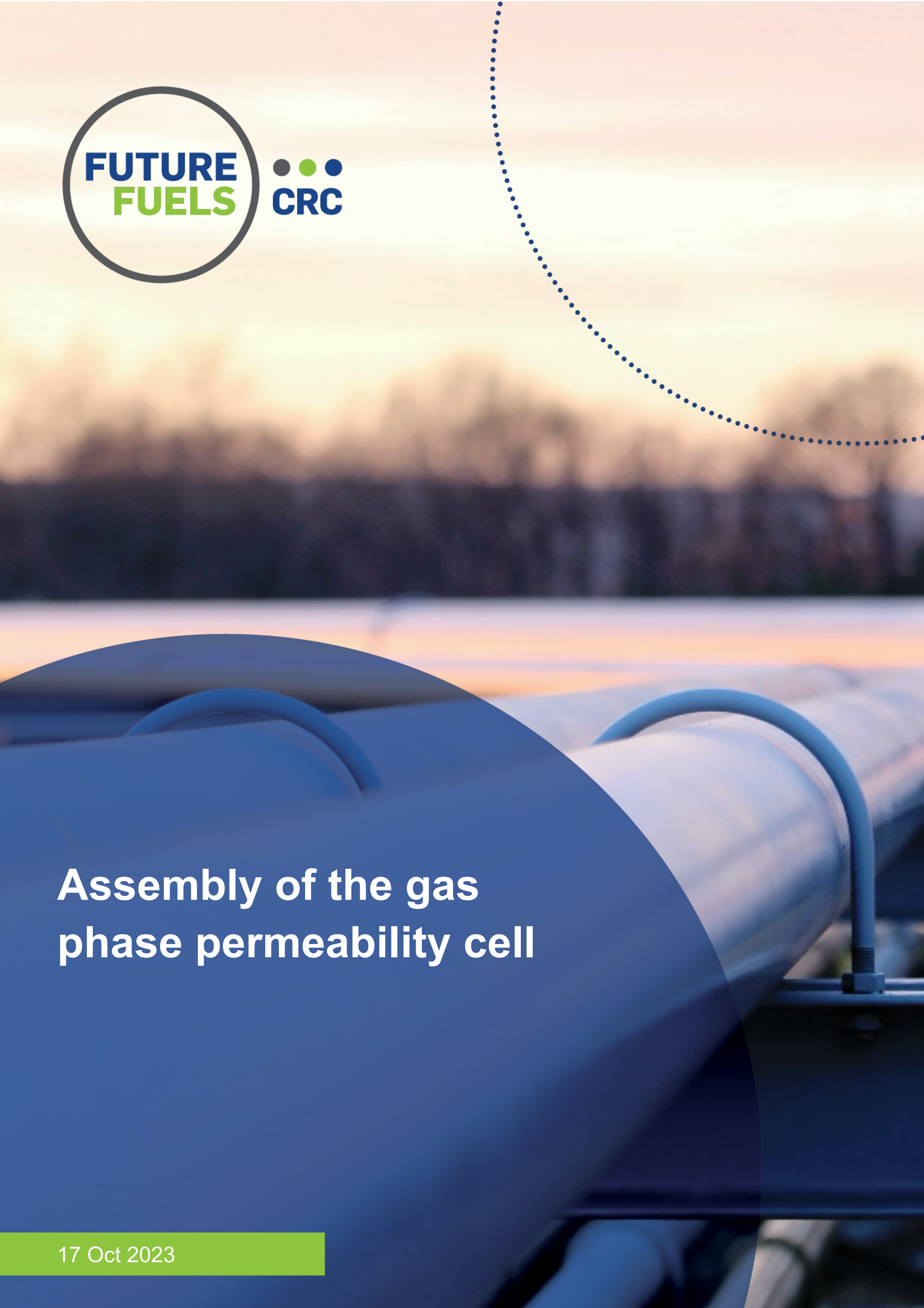

# Assembly of the gas phase permeability cell

17 Oct 2023

Project number: RP3.1-13

Project title: Feasibility of the use of gas phase inhibition of hydrogen embrittlement in gas transmission pipelines carrying hydrogen

Authors: Joshua Hoschke, Maximillian Roethig, Evan Gray, Clotario Tapia-Bastidas, Jeffrey Venezuela, Andrej Atrens

Project team: Andrej Atrens and Evan Gray

Name of project team here

Australian Government
Department of Industry, Science and Resources

AusIndustry
Cooperative Research Centres Program

This work is funded by the Future Fuels CRC, supported through the Australian Government's Cooperative Research Centres Program. We gratefully acknowledge the cash and in-kind support from all our research, government and industry participants.

## IMPORTANT DISCLAIMER



## ACKNOWLEDGEMENT

[Thanks to the researchers working on the project and co-authors of the paper]

| PROJECT INFORMATION | |
|---|---|
| **Project number** | RP3-13 |
| **Project title** | Oxygen inhibition of gaseous hydrogen embrittlement |
| **Research Program** | 3: Network Lifecycle Management |
| **Milestone Report Number** | 2 |
| **Description** | This milestone report describes the gas phase permeation cell and the remaining steps to commission the cell and first experimental studies with the cell. Hydrogen carried by gas transmission pipelines will permeate into the pipeline walls, which can lead to hydrogen embrittlement. This paper details the design of an apparatus which will be used to study the permeation of gaseous hydrogen through pipeline steels at pressures up to 17MPa and temperatures up to 200°C. The results of the permeation tests will be used to (i) characterise the diffusivity and solubility of gaseous hydrogen in pipelines, (ii) equate the conditions in hydrogen embrittlement studies which use electrochemical and gaseous hydrogen charging, and (iii) study the permeation of gaseous hydrogen blended with other gases, particularly trace amounts of oxygen. Permeation studies of hydrogen with oxygen will be used to evaluate the possible use of oxygen as an inhibitor of hydrogen embrittlement. |
| **Research Provider** | The University of Queensland |
| **Project Leader and Team** | Andrejs Atrens, The University of Queensland, Evan Gray Griffith University |
| **Industry Proponent and Advisor Team** | Tawake Rakai, General Manager – Transmission Asset Management, Tim Aujard, Head of Asset Performance, Australian Gas Infrastructure Group |
| **Related Commonwealth Schedule** | RP3.1.1 Reports on the compatibility of current plastic and metallic network materials with future fuels delivered.<br>RP3.1.2 New validated models to determine the long-term performance of materials for fuel transport delivered |
| **Project start/completion date** | **Start Date: 1 February 2022; Completion Date: 1 March 2025,** spending authorized to 12/2026 for orderly project completion because of duration of PhD program of Max Roethig |
| **IP Access** | **Open** – available publicly to all parties outside the CRC |
| **Approved by** | Tawake Rakai, General Manager – Transmission Asset Management, Tim Aujard, Head of Asset Performance, Australian Gas Infrastructure Group |
| **Date of approval** | |

# Table of Contents

# Summary of Report

Hydrogen carried by gas transmission pipelines will permeate into the pipeline walls, which can lead to hydrogen embrittlement. This paper details the design of an apparatus which will be used to study the permeation of gaseous hydrogen through pipeline steels at pressures up to 17MPa and temperatures up to 200°C. The results of the permeation tests will be used to (i) characterise the diffusivity and solubility of gaseous hydrogen in pipelines, (ii) equate the conditions in hydrogen embrittlement studies which use electrochemical and gaseous hydrogen charging, and (iii) study the permeation of gaseous hydrogen blended with other gases, particularly trace amounts of oxygen. Permeation studies of hydrogen with oxygen will be used to evaluate the possible use of oxygen as an inhibitor of hydrogen embrittlement. This report describes the gas phase permeation cell and the remaining steps to commission the cell and being experimental studies with the cell.

## 1. INTRODUCTION

The industry need is that gas transmission pipeline operators require knowledge about safe operating conditions for gas pipelines carrying hydrogen, in terms of the permissible safe operating pressure, and tolerable defect sizes. Otherwise, fractures are expected, with significant collateral damage.

This research will provide critical knowledge regarding the inhibition of hydrogen embrittlement (HE) by small amounts of added gases (O2, CH4, CO, CO2). If 100% inhibition of HE were practical, then the mechanical behaviour of the pipeline steel for a hydrogen carrying pipeline would be exactly the same as that of a gas transmission pipeline with no hydrogen and the operating characteristics would remain the same as at the present time, regardless of the hydrogen content of the gas inside the gas transmission pipeline. The use of this strategy requires in-depth understanding because thermodynamics indicates that the inhibition is a kinetic effect.

This research assesses the feasibility of the use of gas phase inhibition of environmental hydrogen embrittlement for use in gas transmission pipelines carrying hydrogen. The research proposes (i) to study the hydrogen flux entering gas transmission pipeline steels exposed to hydrogen and hydrogen methane mixtures in the presence of small amounts of added gases such as O2, CO, and CO2; and (ii) study the approach to equilibrium solubility of hydrogen in the gas transmission pipeline steels, in particular how quickly equilibrium is approached.

## 2. BODY OF REPORT

Please see attached paper: Hoschke et al Design of a gas permeability apparatus to study oxygen inhibition of hydrogen embrittlement.

## 3. CONCLUSIONS

The paper describes the gas phase permeability apparatus, its design, construction, assembly and proposed use.

## 4. IMPLICATIONS AND RECOMMENDATIONS FOR INDUSTRY

This report is for noting.

## 5. NEXT STEP AND FUTURE WORK

The gas phase permeability cell as described in the attached paper is essentially complete and assembled except for some minor tubing which is to be completed Thursday 19 Oct. The hydrotest has been successfully completed, so that all required documentation has been completed for the submission at Griffith University for safety approvals for the use of the cell with hydrogen. Approval is also awaited for the use of hydrogen in the lab at Griffith Univ, the relevant documentation has been submitted. The electronics is connected, the software is in place, some fine tuning may be needed once the cell is used. Once approval is received for the use of hydrogen in the lab, calibration can be commenced for the various volumes in the apparatus to ensure accurate measurement of the egress hydrogen flux from the specimen during the permeation experiments to ensure accurate measurement of hydrogen diffusivity and hydrogen solubility.

Once calibration has been carried out, the following studies are planned. (i) Measure equilibrium solubility of hydrogen in the gas transmission pipeline steels at room temperature as a function of hydrogen partial pressure from 1 to 200 bar hydrogen in hydrogen and hydrogen methane mixtures in the presence of small amounts of up to 1% of added gases such as O2, CO, and CO2, for the gas pipeline steels used for the hydrogen embrittlement studies at UQ, (ii) Understand the inhibition of hydrogen entry into gas pipeline steels by the presence of the gases such as O2, CO, and CO2.

## 6. REFERENCES

(Please make sure the referencing style is consistent for all milestone reports of the project.)

# Design of a gas permeation apparatus to study oxygen inhibition of hydrogen embrittlement

Joshua Hoschke*, Maximilian Roethig*, Evan Gray†, Clotario Tapia-Bastidas*, Jeffrey Venezuela* and Andrej Atrens*
*School of Mechanical and Mining Engineering, Centre for Advanced Materials Processing and Manufacturing (AMPAM)
The University of Queensland, St Lucia 4072, Australia
Email: Andrejs.Atrens@uq.edu.au
†Queensland Micro- and Nanotechnology Centre
Griffith University, Nathan 4111, Australia

***Abstract*—Hydrogen carried by gas transmission pipelines will permeate into the pipeline walls, which can lead to hydrogen embrittlement. This paper details the design of an apparatus which will be used to study the permeation of gaseous hydrogen through pipeline steels at pressures up to $17\,\mathrm{MPa}$ and temperatures up to $200\,^{\circ}\mathrm{C}$. The results of the permeation tests will be used to (i) characterise the diffusivity and solubility of gaseous hydrogen in pipelines, (ii) equate the conditions in hydrogen embrittlement studies which use electrochemical and gaseous hydrogen charging, and (iii) study the permeation of gaseous hydrogen blended with other gases, particularly trace amounts of oxygen. Permeation studies of hydrogen with oxygen will be used to evaluate the possible use of oxygen as an inhibitor of hydrogen embrittlement.**

***Index Terms*—hydrogen embrittlement, gas permeation, pipeline steel, oxygen inhibition**

## I. Introduction

There has been a large amount of research into hydrogen embrittlement (HE) of pipeline steels. HE in pipelines could be caused by electrochemically generated hydrogen, from sources such as corrosion and cathodic protection [1]–[4], or by gaseous hydrogen within the pipeline. Much of the existing research is motivated by the prospective use of existing steel pipelines to transport gaseous hydrogen, which, when produced from renewable energy sources, would aid in decarbonisation [5]–[7].

Electrochemical charging is frequently used to introduce hydrogen into test specimens when studying HE [8]–[12]. Electrochemical testing can be related to HE caused by gaseous hydrogen provided the relationship between the electrochemical charging conditions and gaseous hydrogen conditions is known. This relationship has been investigated by characterising the hydrogen fugacity in both environments, which can be found using hydrogen permeation experiments or a method of measuring the hydrogen content such as Thermal Desorption Spectroscopy [13]–[16]. In particular, Koren et al. [17] quantified the relationship between gaseous and electrochemical hydrogen charging for X65 pipeline steel, using 3.5% NaCl for electrochemical charging. Data are lacking for other grades of pipeline steels and other electrolytes.

This research has been supported by the Future Fuels Cooperative Research Centre project RP3.1-13.

There is compelling evidence that gaseous HE in metals can be significantly inhibited in hydrogen containing trace amounts of certain gases, particularly oxygen [18]–[21]. This effect has been observed in steels similar to pipeline steels [22]–[25]. This phenomenon is attributed to the preferential adsorption of the inhibiting gas preventing the adsorption of hydrogen to the metal surface, as shown using surface imaging techniques by Germer and MacRae [26] and Holbrook et al. [22], [27].

However, the influence of oxygen on hydrogen diffusion has not been investigated. Ewing and Ubbelohde [28] investigated hydrogen permeation in the presence of oxygen, but their work focused on oxygen inhibiting the desorption of hydrogen from the exit side of a permeation specimen, and as such was not able to study hydrogen diffusion in the metal nor the subsurface hydrogen concentration.

Oxygen inhibition of HE is an attractive strategy for natural gas high-pressure pipelines transporting hydrogen. Is this a feasible strategy on a timescale of tens of years? A deeper quantitative (i.e. timescale, effectiveness, etc.) and qualitative (i.e. type of gases) understanding of gas phase inhibition of HE is needed. The following will provide a deeper understanding of gas phase inhibition of HE.

1) A gas permeation apparatus (GPA) is needed that allows study of the hydrogen flux through a pipeline steel specimen subject to high pressure hydrogen containing a known quantity of added gases, such as $O_2$.
2) A model of the GPA is needed to extract the hydrogen solubility and diffusivity from the measurement of the pressure build-up in the downstream volume.
3) Gas phase permeation experiments need to be carried out with the GPA using pure hydrogen to study the hydrogen solubility and diffusivity of the steel as a function of hydrogen pressure and temperature. This allows gaseous hydrogen charging to be equated to electrochemical charging, and provides a base for comparison with subsequent experiments with added gases. Similar experiments are needed with different gas mixtures to study the influence of the added gas, including the dependence on partial pressure, temperature, steel grade, type and amount of added gas.
4) Measurement of the hydrogen concentration using Ther-

mal Desorption Spectroscopy (TDS) is needed to confirm the GPA data.

5) Use of surface characterisation techniques such as XPS is needed to study the surface mechanisms involved in these inhibition effects.

This paper addresses the first two objectives. The gas-phase permeation apparatus design is described in the following section. An overview over the samples (materials and gases) is given thereafter.

## II. Apparatus Design

Permeation experiments study the permeation of hydrogen through a membrane of the material of interest. The transport parameters (diffusivity, solubility, and permeability) are evaluated from the hydrogen flux through the specimen.

Typical hydrogen permeation methods include methods that use (i) electrochemical hydrogen charging and detection, (ii) gas phase charging and detection, and (iii) gas phase charging with electrochemical detection [29]. In a typical permeation experiment, the inlet hydrogen flux (as determined by the current or pressure) is quickly increased or decreased, and the exit hydrogen flux is recorded over time. The inlet flux over time is represented by a step function, while the exit flux resembles a sigmoid function. A single change in the inlet flux, and the corresponding change in the exit flux, is referred to as a permeation transient [30]. Multiple transients can be performed successively to collect multiple data points for the steel's properties.

Further distinction between hydrogen permeation methods can be made by the governing boundary conditions [31]. In an ideal case, the charging condition (e.g. pressure) remains constant and a steady-state flux is established. In contrast, in a gas phase permeation rig, a fixed volume on the downstream side of the permeation membrane results in downstream pressure increasing over time, and a fixed upstream volume results in a decreasing upstream pressure. This causes the flux to be in a transient state throughout the experiment.

This proposed gas permeation apparatus (GPA) uses high-pressure hydrogen gas charging, closely replicating the pressures expected in gas pipelines carrying hydrogen. The approach enables the study of the influence of different hydrogen gas blends and added impurities by injection of the proposed gas phase inhibitors. Finally, gas phase permeation allows the determination of the hydrogen solubility in the steel membrane as a function of the hydrogen partial pressure.

A schematic of the GPA is presented in Fig. 1. Table I gives an overview of the sections and their associated valves. There are gas inlets for hydrogen, methane, oxygen, and carbon monoxide. To create a gas mixture, each constituent gas is fed into one of the two sample cylinders ($Vref,1$ and $Vref,2$) at a desired pressure. After the first cylinder is charged, the manifold is evacuated such that the second cylinder is not contaminated. Once both cylinders are charged, Valve 7a and Valve 7b are opened and the gas mixture is created in the manifold and the two sample cylinders. This produces a volume $>300\,\mathrm{cm}^3$ from which the upstream section can be charged multiple times.

TABLE I: Sections and partitioning of the GPR. Numbers refer to valve numbers in Fig. 1 (not including pressure relief valves as they don't serve control purpose).

| Group | No. | Section | Enclosed by |
|---|---|---|---|
| Supply | 1 | Metal-Hydride Sample Cylinder | 1d |
| | 2 | Hydrogen Inlet | 1a, 1b, 1d |
| | 3 | Oxygen Inlet | 2a, 2b |
| | 4 | Carbon Monoxide Inlet | 3a, 3b |
| | 5 | Methane Inlet | 4a, 4b |
| Manifold | 6 | Manifold | 1b, 2b, 3b, 4b, 5, 6, 7a, 7b, 9 |
| | 7a | Reference Volume 1 | 7a |
| | 7b | Reference Volume 2 | 7b |
| Upstream | 8a | Upstream High Pressure | 9, 11a, 11b, 12a |
| | 8b | Upstream Permeation Cell | 11a, Cell |
| | 8c | Upstream Low Pressure | 11b |
| Downstream | 9a | Downstream Manifold | Cell, 13a, 13b, 13c |
| | 9b | Downstream Low Pressure | 13b |
| | 9c | Downstream High Pressure | 13c, 14 |
| Vacuum | 10 | Vacuum Outlet | 6, 12b, 14 |

The upstream pressure can be precisely controlled to a desired pressure using a needle valve (Valve 9).

The permeation cell holds the disc specimen as shown in Fig. 3. At the beginning of each experiment, a vacuum is created downstream of the specimen, and high-pressure gas is introduced into from the upstream section. This can result in pressure gradients across the specimen of up to $200\,\mathrm{bar}$. The minimum thickness of a circular plate with fixed edges is calculated using [32]

$$t = 2r\sqrt{\frac{0.19P}{\sigma}} \tag{1}$$

where $r$ is the radius of the disc, $P$ is the applied pressure and $\sigma$ the allowable stress. A steel disc specimen for testing in the GPA has a thickness of $4\,\mathrm{mm}$ and an exposed radius of $11\,\mathrm{mm}$, which results in the maximum stress remaining below half of the yield strength in the softest steel to be tested (X42, 290 MPa). Typically, hydrogen does not significantly reduce the yield strength of steel [6], [33]. For a pure annealed iron specimen, the upstream pressure may not exceed $50\,\mathrm{bar}$.

The hydrogen flux is evaluated from the pressure increase in the downstream vacuum section using a high-accuracy pressure transmitter (MKS Baratron AA04A). Additionally, the specimen temperature can be controlled by a band heater attached to the permeation cell, allowing the study of the influence of temperature on hydrogen diffusion and solubility. A vacuum pump is used to evacuate the system, and a helium inlet line is used to purge the system. The design of the GPA allows for evacuating specific sections (e.g. manifold for gas mixing) or the whole system (i.e. evacuation before or after individual runs).

The maximum pressure and temperature ratings are dictated by the weakest link. All tubing, piping, and the double-ended sample cylinders are rated $\geq 344\,\mathrm{bar}$ at room temperature. The maximum temperature is $537\,^{\circ}\mathrm{C}$. Diaphragm valves are rated $209\,\mathrm{bar}$ at $65\,^{\circ}\mathrm{C}$, whereas high purity diaphragm valves, used in close proximity to the permeation cell, may reach pressures of up to $241\,\mathrm{bar}$ at room temperature and $192\,\mathrm{bar}$ at $121\,^{\circ}\mathrm{C}$. Most sections only experience room temperature. To stay within

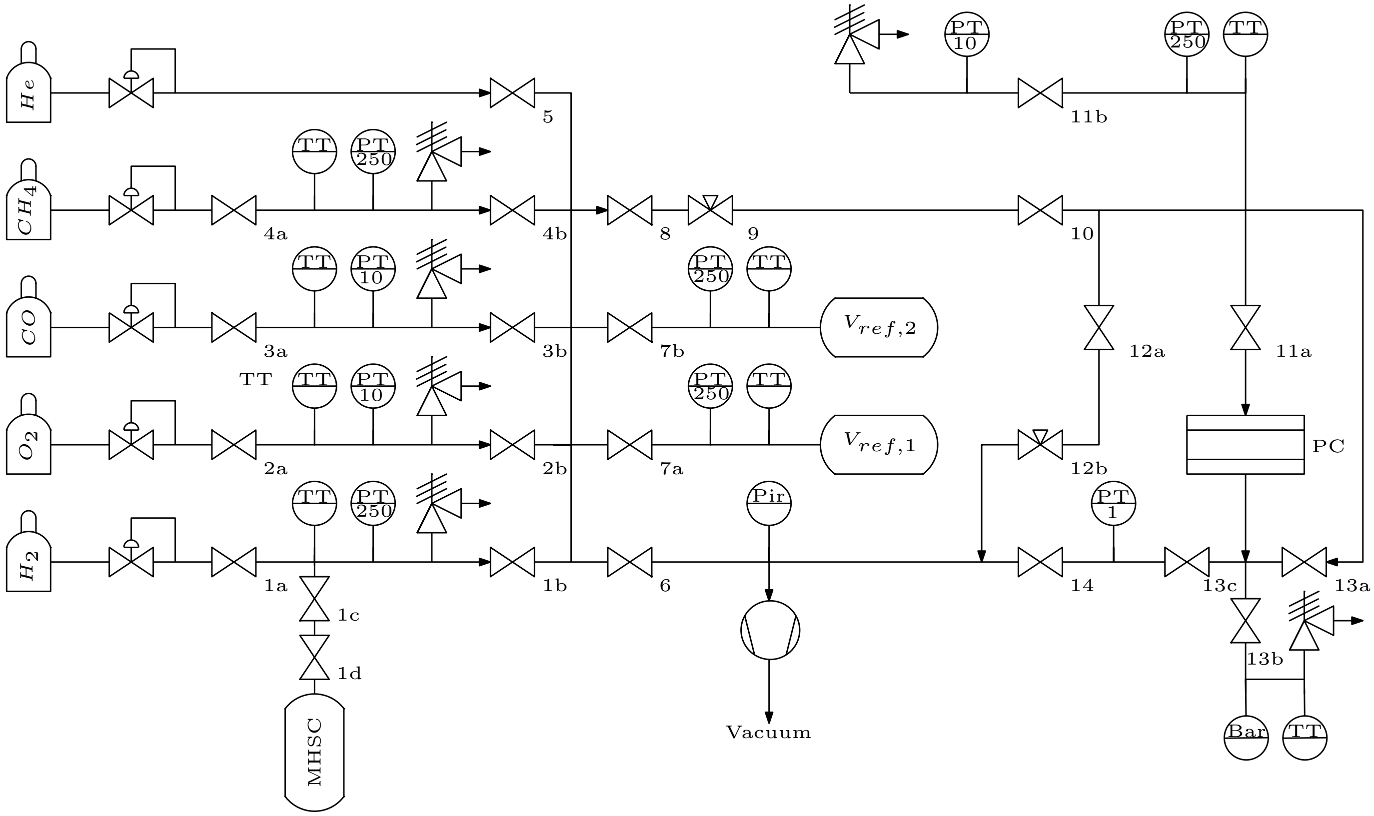


Fig. 1: Piping and Instrumentation Diagram of the GPR. The integrated thermocouples in the permeation cell are not drawn. Arrows depict the main directions of gas flow. Where different directions are possible, no arrows are shown.

these limitations, only final pressures of approximately $120\,\mathrm{bar}$ to $150\,\mathrm{bar}$, depending on the gas blend, are feasible. After mixture preparation in sections 7, 8 and 9, gas is expanded into the upstream compartment. While pressures in the mentioned mixing sections may only safely reach $209\,\mathrm{bar}$, the pressure after expansion decreases, which conforms to the temperature-pressure rating of the surrounding valves.

At the beginning of each experiment, gases are sourced from cylinders through entry sections (sections 3, 4 or 5 in Table I). Hydrogen, as the main constituent of every gas mixture, is an exception, as hydrogen is supplied by a metal hydride sample cylinder (MHSC). In order to assess the effects of added gases for each experiment, the sourced hydrogen needs to contain as little impurities as possible. Usually, hydrogen fed from conventional gas cylinders for laboratory use does not meet purity requirements. Furthermore, gas cylinder pressures may be too low. An MHSC effectively functions as a compressor by absorbing hydrogen at low temperatures and desorbing it upon heating (see fig. 2). In a laboratory, an MHSC acts as a good alternative to a conventional compressor or gas cylinder. A single-stage MHSC can be used for periodic charging and discharging, and does not involve any moving parts. Additionally, hydrogen gas can be reused between experiments by cooling and reheating the MHSC, and, due to the closed design, contamination is less likely inside the apparatus. Furthermore, desorption of hydrogen from the metal hydride produces high-purity gas, suitable for permeation studies. For a given temperature, absorption is driven by the difference between equilibrium pressure and supply pressure. Likewise, desorption is driven by the difference between equilibrium pressure and discharge pressure. The equilibrium pressure is described by the van 't Hoff equation [34]–[36]

$$\ln P_{eq} = \frac{\Delta H}{RT} - \frac{\Delta S}{R} \tag{2}$$

where $P_{eq}$ is the equilibrium pressure at temperature $T$, $\Delta H$ and $\Delta S$ are material-dependent enthalpy and entropy of hydride formation with respect to a standard state, and $R$ is the universal gas constant. This equation is an ideal approximation, ignoring the hysteresis that occurs between absorption and desorption. Fig. 2b indicates that hydrogen is produced at an almost constant pressure. Isotherm 1 is a lower temperature ($T_L$) and isotherm 2 is a higher temperature ($T_H$). When heat is rejected from the MHSC, the equilibrium pressure decreases. As long as the supply pressure exceeds the pressure at the lower operating point B ($P_l$, $T_L$), the MHSC is charged, forming metal hydride. Vice versa, the decomposition takes place when heating to a higher operating point C ($P_h$, $T_H$). The available amount of hydrogen equals the change of concentration $\Delta c$ between points B and C and is called the reversible storage capacity [36]. Identifying the operating pressures, temperatures, and storage capacity allows for the selection of a suitable material. Here $LaNi_5$ is used. Heat is applied using a heat gun. The

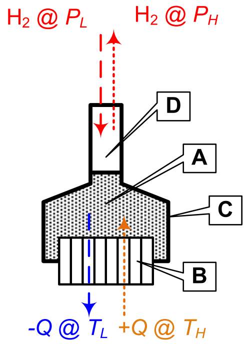


(a) Layout of a single-staged periodically operated compressor, with metal hydride (A), heat source/sink (B), pressure vessel (C) and piping including a gas filter (D). The dashed arrow corresponds to path A in Fig. 2b, whereas the dotted arrow equates to path D.

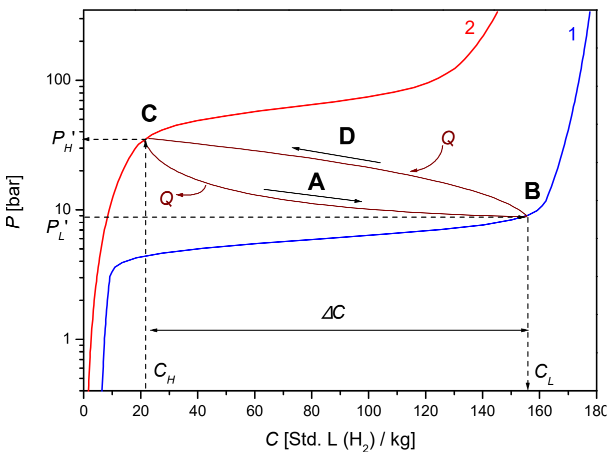


(b) Schematic illustration of two pressure-composition isotherms for a metal hydride. Isotherm 1 is at 20 °C, and isotherm 2 is at 150 °C. Paths A and D represent cyclical absorption and desorption where heat is removed or supplied, respectively. Points B and C depict equilibria states.

Fig. 2: The design and operation of metal hydride compressors. Reproduced from Lototskyy et al. [35] with permission.

temperature-pressure rating of the MHSC vessel is 210 bar at 260 °C, which is higher than the high operating point.

## III. Environments and Materials

Annealed pure iron is to be used for initial test runs on the GPA. The transport parameters of iron are readily available in the literature, which makes it easier to assess the accuracy of the set-up. In subsequent experiments three different pipeline steels (X42, X65 and X70) will be used as permeation membranes to study their hydrogen solubility and diffusivity when charged by high-pressure hydrogen. Sample materials will be cut into discs with a diameter of 32 mm and a thickness of 4 mm to be loaded into the permeation cell.

The gas mixtures are summarised in Table II. Permeation tests in pure hydrogen are expected to produce the highest diffusion coefficients. Therefore, they represent a baseline for gas mixtures that are assumed to inhibit hydrogen diffusion. Gas transmission pipelines that are to be converted to carry

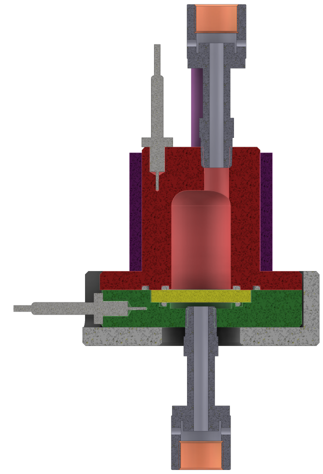

Fig. 3: Detailed drawing of the permeation cell. The disc specimen is coloured yellow. The housing (red and green) is made of stainless steel and enclosed by a band heater (purple) to control the specimen's temperature. Ceramic insulation (dark grey) limits heat loss and steep temperature gradients across the permeation cell.

pure hydrogen will exhibit these conditions. Methane-hydrogen mixtures of various hydrogen contents are investigated as they represent prospective operating conditions where hydrogen is blended into natural gas pipelines. In later experiments small amounts of oxygen or carbon monoxide will be blended into pure hydrogen. These experiments will study the feasibility of the use of these gases as hydrogen embrittlement inhibitors. Future investigation of mixtures including other gases is possible by simply switching the gas inlet connections to different gas cylinders.

Hydrogen has a lower explosive limit (LEL) of 4 vol.% and an upper explosive limit (UEL) of 75 vol.% while methane's LEL is 5 vol.% and UEL is 15 vol.%. All sample mixtures are outside these ranges and are thereby too lean to be flammable.

## IV. Data Analysis

Consider that the specimen is exposed to pure hydrogen in the upstream chamber, and that the upstream hydrogen pressure is increased from 0 MPa to 10 MPa essentially instantaneously

TABLE II: Investigated gas mixtures. Target compositions in volume fraction and partial pressure are listed. Note that 0.001 vol.% is equal to 10 vppm.

| Mixtures | $H_2$ vol.% | $H_2$ bar | $CH_4$ vol.% | $CH_4$ bar | $O_2$ vol.% | $O_2$ bar | CO vol.% | CO bar | $p_{Total}$ (bar) |
|---|---|---|---|---|---|---|---|---|---|
| Pure $H_2$ | 100 | 170 | 0 | 0 | 0 | 0 | 0 | 0 | 170 |
| $CH_4$ based | 5 | 7.5 | 95 | 142.5 | 0 | 0 | 0 | 0 | 150 |
| | 25 | 37.5 | 75 | 112.5 | 0 | 0 | 0 | 0 | 150 |
| $O_2$ based | 99.99 | 149.985 | 0 | 0 | 0.01 | 0.015 | 0 | 0 | 150 |
| | 99.999 | 119.9988 | 0 | 0 | 0.001 | 0.0012 | 0 | 0 | 120 |
| CO based | 99.99 | 149.985 | 0 | 0 | 0 | 0 | 0.01 | 0.015 | 150 |
| | 99.999 | 119.9988 | 0 | 0 | 0 | 0 | 0.001 | 0.0012 | 120 |

by opening the upstream valve. The hydrogen flux, $J$, has units $\mathrm{mol/m^2/s}$ and is given by

$$J(t) = \frac{dn}{dt}\frac{1}{A} \tag{3}$$

where $n$ is the amount of hydrogen, $t$ is time, and $A$ is the area from which hydrogen is egressing. If the boundary conditions are that of constant hydrogen concentration on the entry side, and 0 hydrogen concentration on the exit side, the flux is expected to be given by [30], [37]

$$\frac{J_t - J_0}{J_\infty - J_0} = \frac{2L}{\sqrt{\pi D t}} \sum_{n=0}^{\infty} \exp\left(-\frac{(2n+1)^2 L^2}{4Dt}\right) \tag{4}$$

where $J_0$ is the flux before the transient (in this case 0), $J_\infty$ is the steady-state value which the flux approaches, $L$ is the thickness of the specimen, $D$ is the diffusion coefficient, and $t$ is the time since the transient began. The pressure, $P$, in the downstream chamber is related to the flux by

$$\frac{dP}{dt} = J(t)\frac{AZRT}{V} \tag{5}$$

where $Z$ is the compressibility factor, $R$ is the gas constant, $T$ is the temperature, and $V$ is the downstream volume. Combining (4) and (5) gives

$$\frac{\left(\frac{dp}{dt}\right)_t - \left(\frac{dp}{dt}\right)_0}{\left(\frac{dp}{dt}\right)_\infty - \left(\frac{dp}{dt}\right)_0} = \frac{AZRT}{V}\frac{2L}{\sqrt{\pi D t}} \sum_{n=0}^{\infty} \exp\left(-\frac{(2n+1)^2 L^2}{4Dt}\right) \tag{6}$$

Fitting the shape of this theoretical pressure transient to the experimentally measured time derivative of the pressure enables measurement of the effective diffusion coefficient of the steel. The hydrogen concentration in the specimen in equilibrium with the applied hydrogen pressure is derived from Fick's first law of diffusion and is given by [38]

$$C_\mathrm{H} = \frac{J_\infty L}{D} \tag{7}$$

$$C_\mathrm{H} = \frac{\left(\frac{dP}{dt}\right)_\infty V \cdot L}{AZRT \cdot D} \tag{8}$$

Equations 6 and 8 can be used to determine the effective diffusivity and hydrogen concentration in the steel. Similarly, consider that the upstream chamber contains hydrogen with 1000 vppm oxygen. Consider increasing the pressure essentially instantaneously from 0 bar to 100 bar. The oxygen is expected to inhibit the ingress of hydrogen into the specimen. The resulting hydrogen permeation transient can be fitted to Equation (6) and used to predict the hydrogen diffusion properties when inhibited by oxygen, including the time to steady-state flux, $t_{\infty,\mathrm{O}}$ and the hydrogen concentration, $C_{\mathrm{H,O}}$. The quantities $t_{\infty,\mathrm{O}}/t_\infty$ and $C_{\mathrm{H,O}}/C_\mathrm{H}$ can be used to quantify the effectiveness of the oxygen inhibition of gaseous hydrogen embrittlement.

As permeation in the GPA occurs, a small amount of hydrogen is transferred from the upstream section to the downstream section, resulting in the upstream pressure slightly decreasing and the downstream pressure slightly increasing. This causes the entry and exit concentrations to vary over time. As such the boundary conditions differ from those given in McBreen, Nonis and Beck [30], and Equations (6) and (8) are not entirely accurate to gaseous permeation. However, the error is expected to be small. In future work we plan to evaluate this error, and derive new governing equations from these varying boundary conditions.

## V. Summary

The gas permeation apparatus will be used to study hydrogen permeation through pipeline steels. Experiments with the high-pressure hydrogen gas can be equated to permeation studies using cathodic charging by correlating the subsurface hydrogen concentrations [13], [21], [39]. Gas impurities, including oxygen, will be added to the hydrogen to study their influence on hydrogen diffusion, allowing assessment of the feasibility of gas-phase inhibition of HE to protect steel pipelines carrying hydrogen.


## Acknowledgement

This work is funded by the Future Fuels CRC research projects RP3.1-13 and RP3.1-10, supported through the Australian Government's Cooperative Research Centres Program. Sam Grieve is thanked for his design of the permeation cell and his assistance in the design of the gas permeation apparatus.


## References


[1] M. Cabrini, S. Lorenzi, S. Pellegrini, and T. Pastore, "Environmentally assisted cracking and hydrogen diffusion in traditional and high-strength pipeline steels," *Corrosion Reviews*, vol. 33, no. 6, pp. 529–545, Nov. 2015. [Online]. Available: https://www.degruyter.com/document/doi/10.1515/corrrev-2015-0051/html

[2] G. Ghosh, P. Rostron, R. Garg, and A. Panday, "Hydrogen induced cracking of pipeline and pressure vessel steels: A review," *Engineering Fracture Mechanics*, vol. 199, pp. 609–618, Aug. 2018. [Online]. Available: https://linkinghub.elsevier.com/retrieve/pii/S0013794418301024

[3] E. Ohaeri, U. Eduok, and J. Szpunar, "Hydrogen related degradation in pipeline steel: A review," *International Journal of Hydrogen Energy*, vol. 43, no. 31, pp. 14 584–14 617, Aug. 2018. [Online]. Available: https://linkinghub.elsevier.com/retrieve/pii/S0360319918318767

[4] E. G. Ohaeri, W. Qin, and J. Szpunar, "A critical perspective on pipeline processing and failure risks in hydrogen service conditions," *Journal of Alloys and Compounds*, vol. 857, p. 158240, Mar. 2021. [Online]. Available: https://linkinghub.elsevier.com/retrieve/pii/S092583882034603X

[5] N. Nanninga, A. Slifka, Y. Levy, and C. White, "A Review of Fatigue Crack Growth for Pipeline Steels Exposed to Hydrogen," *Journal of Research of the National Institute of Standards and Technology*, vol. 115, no. 6, pp. 437–452, 2010. [Online]. Available: https://www.ncbi.nlm.nih.gov/pmc/articles/PMC4548866/

[6] J. Hoschke, M. F. W. Chowdhury, J. Venezuela, and A. Atrens, "A review of hydrogen embrittlement in gas transmission pipeline steels," *Corrosion Reviews*, vol. 41, no. 3, Mar. 2023. [Online]. Available: https://www.degruyter.com/document/doi/10.1515/corrrev-2022-0052/html

[7] G. Jia, M. Lei, M. Li, W. Xu, R. Li, Y. Lu, and M. Cai, "Hydrogen embrittlement in hydrogen-blended natural gas transportation systems: A review," *International Journal of Hydrogen Energy*, p. S0360319923020967, May 2023. [Online]. Available: https://linkinghub.elsevier.com/retrieve/pii/S0360319923020967

[8] B. Gu, J. Luo, and X. Mao, "Hydrogen-Facilitated Anodic Dissolution-Type Stress Corrosion Cracking of Pipeline Steels in Near-Neutral pH Solution," *Corrosion*, vol. 55, no. 01, Jan. 1999.

[9] D. Hardie, E. Charles, and A. Lopez, "Hydrogen embrittlement of high strength pipeline steels," *Corrosion Science*, vol. 48, no. 12, pp. 4378–4385, Dec. 2006. [Online]. Available: https://linkinghub.elsevier.com/retrieve/pii/S0010938X06000710

[10] C. Dong, Z. Liu, X. Li, and Y. Cheng, "Effects of hydrogen-charging on the susceptibility of X100 pipeline steel to hydrogen-induced cracking," *International Journal of Hydrogen Energy*, vol. 34, no. 24, pp. 9879–9884, Dec. 2009. [Online]. Available: https://linkinghub.elsevier.com/retrieve/pii/S0360319909015304

[11] R. Wang, "Effects of hydrogen on the fracture toughness of a X70 pipeline steel," *Corrosion Science*, vol. 51, no. 12, pp. 2803–2810, Dec. 2009. [Online]. Available: https://linkinghub.elsevier.com/retrieve/pii/S0010938X09003618

[12] A. Alhussein, J. Capelle, J. Gilgert, S. Dominiak, and Z. Azari, "Influence of sandblasting and hydrogen on tensile and fatigue properties of pipeline API 5L X52 steel," *International Journal of Hydrogen Energy*, vol. 36, no. 3, pp. 2291–2301, Feb. 2011. [Online]. Available: https://linkinghub.elsevier.com/retrieve/pii/S0360319910022962

[13] A. Atrens, D. Mezzanotte, N. F. Fiore, and M. A. Genshaw, "Electrochemical studies of hydrogen diffusion and permeability in Ni," *Corrosion Science*, vol. 20, no. 5, pp. 673–684, Jan. 1980. [Online]. Available: https://www.sciencedirect.com/science/article/pii/0010938X8090102X

[14] J. Venezuela, E. Gray, Q. Liu, Q. Zhou, C. Tapia-Bastidas, M. Zhang, and A. Atrens, "Equivalent hydrogen fugacity during electrochemical charging of some martensitic advanced high-strength steels," *Corrosion Science*, vol. 127, pp. 45–58, Oct. 2017. [Online]. Available: https://linkinghub.elsevier.com/retrieve/pii/S0010938X17304572

[15] J. Venezuela, C. Tapia-Bastidas, Q. Zhou, T. Depover, K. Verbeken, E. Gray, Q. Liu, Q. Liu, M. Zhang, and A. Atrens, "Determination of the equivalent hydrogen fugacity during electrochemical charging of 3.5NiCrMoV steel," *Corrosion Science*, vol. 132, pp. 90–106, Mar. 2018. [Online]. Available: https://linkinghub.elsevier.com/retrieve/pii/S0010938X17319595

[16] Q. Liu, E. Gray, J. Venezuela, Q. Zhou, C. Tapia-Bastidas, M. Zhang, and A. Atrens, "Equivalent Hydrogen Fugacity during Electrochemical Charging of 980DP Steel Determined by Thermal Desorption Spectroscopy," *Advanced Engineering Materials*, vol. 20, no. 1, p. 1700469, Jan. 2018. [Online]. Available: https://onlinelibrary.wiley.com/doi/10.1002/adem.201700469

[17] E. Koren, C. M. H. Hagen, D. Wang, X. Lu, R. Johnsen, and J. Yamabe, "Experimental comparison of gaseous and electrochemical hydrogen charging in X65 pipeline steel using the permeation technique," *Corrosion Science*, vol. 215, p. 111025, May 2023. [Online]. Available: https://www.sciencedirect.com/science/article/pii/S0010938X23000677

[18] J. D. Frandsen and H. L. Marcus, "Environmentally assisted fatigue crack propagation in steel," *Metallurgical Transactions A*, vol. 8, no. 2, pp. 265–272, Feb. 1977. [Online]. Available: http://link.springer.com/10.1007/BF02661639

[19] P. Deimel, H. Leonhard, and E. Sattler, "Characterization of the influence of high-pressure hydrogen gas on the ductility of the steel 15 MnNi 6 3," *International Journal of Hydrogen Energy*, vol. 18, no. 4, pp. 313–318, Apr. 1993. [Online]. Available: https://linkinghub.elsevier.com/retrieve/pii/036031999390045C

[20] K. Kussmaul, "Fracture mechanical behaviour of the steel 15 MnNi 6 3 in argon and in high pressure hydrogen gas with admixtures of oxygen," *International Journal of Hydrogen Energy*, vol. 23, no. 7, pp. 577–582, Jul. 1998. [Online]. Available: https://linkinghub.elsevier.com/retrieve/pii/S0360319997001043

[21] A. Atrens, E. Gray, J. Venezuela, J. Hoschke, and M. Roethig, "Feasibility of the Use of Gas Phase Inhibition of Hydrogen Embrittlement in Gas Transmission Pipelines Carrying Hydrogen: A Review," *JOM*, Oct. 2022. [Online]. Available: https://doi.org/10.1007/s11837-022-05559-8

[22] J. Holbrook, E. Collings, H. Cialone, and E. Drauglis, "Hydrogen degradation of pipeline steels: Final report," Battelle Columbus Laboratories, Tech. Rep. BNL-52049, 7122938, ON: DE87005585, Mar. 1986. [Online]. Available: https://www.osti.gov/servlets/purl/7122938/

[23] H. J. Cialone and J. H. Holbrook, "Sensitivity of Steels to Degradation in Gaseous Hydrogen," in *Hydrogen Embrittlement: Prevention and Control*, L. Raymond, Ed. 100 Barr Harbor Drive, PO Box C700, West Conshohocken, PA 19428-2959: ASTM International, Jan. 1988, pp. 134–134–19. [Online]. Available: http://www.astm.org/doiLink.cgi?STP45297S

[24] B. Somerday, P. Sofronis, K. Nibur, C. San Marchi, and R. Kirchheim, "Elucidating the variables affecting accelerated fatigue crack growth of steels in hydrogen gas with low oxygen concentrations," *Acta Materialia*, vol. 61, no. 16, pp. 6153–6170, Sep. 2013. [Online]. Available: https://linkinghub.elsevier.com/retrieve/pii/S1359645413005016

[25] R. Komoda, M. Kubota, S. Yoshida, A. Staykov, P. Ginet, F. Barbier, and J. Furtado, "Inhibition of Hydrogen Embrittlement of Cr-Mo Steel by the Addition of Impurities to Hydrogen Environment and the Effect of Material Strength," in *Proceedings of the Twenty-eighth (2018) International Ocean and Polar Engineering Conference*. OnePetro, Jun. 2018. [Online]. Available: https://onepetro.org/ISOPEIOPEC/proceedings-abstract/ISOPE18/All-ISOPE18/20777

[26] L. H. Germer and A. U. MacRae, "Adsorption of Hydrogen on a (110) Nickel Surface," *The Journal of Chemical Physics*, vol. 37, no. 7, pp. 1382–1386, Oct. 1962. [Online]. Available: https://doi.org/10.1063/1.1733293

[27] J. Holbrook, H. Cialone, E. Collings, E. Drauglis, P. Scott, and M. Mayfield, "Control of hydrogen embrittlement of metals by chemical inhibitors and coatings," in *Gaseous Hydrogen Embrittlement of Materials in Energy Technologies*. Elsevier, 2012, pp. 129–153. [Online]. Available: https://linkinghub.elsevier.com/retrieve/pii/B9780857095367500052

[28] V. C. Ewing and A. R. J. P. Ubbelohde, "Hydrogenation through metal septa," *Proceedings of the Royal Society of London. Series A. Mathematical and Physical Sciences*, vol. 230, no. 1182, pp. 301–311, Jun. 1955, publisher: Royal Society. [Online]. Available: https://royalsocietypublishing.org/doi/10.1098/rspa.1955.0133

[29] W. Zhao, T. Zhang, Y. Zhao, J. Sun, and Y. Wang, "Hydrogen permeation and embrittlement susceptibility of X80 welded joint under high-pressure coal gas environment," *Corrosion Science*, vol. 111, pp. 84–97, Oct. 2016. [Online]. Available: https://linkinghub.elsevier.com/retrieve/pii/S0010938X16301809

[30] J. McBreen, L. Nonis, and W. Beck, "A Method for Determination of the Permeation Rate of Hydrogen Through Metal Membranes," *Journal of The Electrochemical Society*, vol. 113, no. 11, p. 1218, Nov. 1966, publisher: IOP Publishing. [Online]. Available: https://iopscience.iop.org/article/10.1149/1.3087209/meta

[31] K. Setnickova, L. Jiriste, M. Maly, R. Petrickovic, H. H. Tseng, and P. Uchytil, "An approach for evaluating gas sorption in polymer matrix membranes based on balancing incoming and outgoing membrane mass fluxes," *Journal of Membrane Science*, vol. 661, p. 120867, Nov. 2022. [Online]. Available: https://www.sciencedirect.com/science/article/pii/S0376738822006123

[32] M. H. Jawad, "Bending of Circular Plates," in *Stress in ASME Pressure Vessels, Boilers, and Nuclear Components*. ASME-Wiley, Nov. 2017. [Online]. Available: https://asmedigitalcollection.asme.org/ebooks/book/18/chapter/788/Bending-of-Circular-Plates

[33] M. R. Louthan, "Hydrogen Embrittlement of Metals: A Primer for the Failure Analyst," *Journal of Failure Analysis and Prevention*, vol. 8, no. 3, pp. 289–307, Jun. 2008. [Online]. Available: http://link.springer.com/10.1007/s11668-008-9133-x

[34] E. M. Gray and C. J. Webb, "Metal-hydride hydrogen compressors for laboratory use," *Journal of Physics: Energy*, vol. 2, no. 3, p. 034004, Jul. 2020, publisher: IOP Publishing. [Online]. Available: https://dx.doi.org/10.1088/2515-7655/ab9314

[35] M. V. Lototskyy, V. A. Yartys, B. G. Pollet, and R. C. Bowman, "Metal hydride hydrogen compressors: A review," *International Journal of Hydrogen Energy*, vol. 39, no. 11, pp. 5818–5851, Apr. 2014. [Online]. Available: https://www.sciencedirect.com/science/article/pii/S0360319914002389

[36] D. P. Broom, "Hydrogen Sorption Properties of Materials," in *Hydrogen Storage Materials: The Characterisation of Their Storage Properties*, ser. Green Energy and Technology, D. P. Broom, Ed. London: Springer, 2011, pp. 61–115. [Online]. Available: https://doi.org/10.1007/978-0-85729-221-6_3

[37] J. Venezuela, Q. Zhou, Q. Liu, M. Zhang, and A. Atrens, "Influence of hydrogen on the mechanical and fracture properties of some martensitic advanced high strength steels in simulated service conditions," *Corrosion Science*, vol. 111, pp. 602–624, Oct. 2016. [Online]. Available: https://www.sciencedirect.com/science/article/pii/S0010938X16302633

[38] J. Crank, *The mathematics of diffusion*, 2nd ed. Oxford, [Eng]: Clarendon Press, 1975.

[39] Q. Liu, A. D. Atrens, Z. Shi, K. Verbeken, and A. Atrens, "Determination of the hydrogen fugacity during electrolytic charging of steel," *Corrosion Science*, vol. 87, pp. 239–258, Oct. 2014. [Online]. Available: https://www.sciencedirect.com/science/article/pii/S0010938X14002893

FUTURE FUELS CRC

# Future Fuels CRC

Enabling the Decarbonisation of Australia's Energy Networks


www.futurefuelscrc.com

info@futurefuelscrc.com



Australian Government
Department of Industry, Science and Resources

AusIndustry
Cooperative Research Centres Program